Enhanced four-wave mixing via photonic bandgap coupled defect resonances

S. Blair
University of Utah, Department of Electrical and Computer Engineering
Salt Lake City, UT 84112
blair@ece.utah.edu

Abstract: Frequency conversion efficiency via four-wave mixing in coupled 1-D photonic crystal defect structures is studied numerically. In structures where all interacting frequencies coincide with intraband defect resonances, energy conversion efficiencies greater than 5% are predicted. Because the frequency spacings are determined by the free-spectral range, thereby requiring long defects for small spacings using intraband resonances, four-wave mixing using coupled-defect miniband resonances in more compact structures is also studied. Conversion efficiencies of greater than 1% are obtained in this case.

OCIS codes: (190.4380) Four-wave mixing, (230.5750) Resonators.

References and links

1. E. Yablonovitch "Inhibited spontaneous emission in solid-state physics and electronics," Phys. Rev. Lett. **58,** 2059–2062 (1987).
2. S. John "Strong localization of photons in certain disordered dielectric superlattices," Phys. Rev. Lett. **58,** 2486–2489 (1987).
3. T. F. Krauss "Planar photonic crystal waveguide devices for integrated optics," Physica Status Solidi A **197,** 688–702 (2003).
4. M. Soljacic, C. Luo, J. D. Joannopoulos, and S. Fan "Nonlinear photonic crystal microcavities for optical integration," Opt. Lett. **28,** 637–639 (2003).
5. O. Painter, R. K. Lee, A. Scherer, A. Yariv, J. D. O'Brien, P. D. Dapkus, and I. Kim "Two-dimensional photonic band-gap defect mode laser," Science **284,** 1819–1821 (1999).
6. D. M. Pustai, A. Sharkawy, S. Shouyuan, and D. W. Prather "Tunable photonic crystal microcavities," Appl. Optics **41,** 5574–5579 (2002).
7. J. S. Foresi, P. R. Villeneuve, J. Ferrera, E. R. Thoen, G. Steinmeyer, S. Fan, J. D. Joannopoulos, L. C. Kimerling, H. I. Smith, and E. P. Ippen "Photonic-bandgap microcavities in optical waveguides," Nature **390,** 143–154 (1997).
8. A. S. Jugessur, P. Pottier, and R. M. D. L. Rue "Engineering the filter response of photonic crystal microcavity filters," Opt. Express **12,** 1304–1312 (2004).
9. N. Stefanou and A. Modinos "Impurity bands in photonic insulators," Phys. Rev. B **57,** 12127–12133 (1998).
10. A. Yariv, Y. Xu, R. K. Lee, and A. Scherer "Coupled-resonator optical waveguides: a proposal and analysis," Opt. Lett. **24,** 711–713 (1999).
11. R. Houdre, and U. Oesterle "Miniband transmission in a photonic crystal coupled-resonator optical waveguide," Opt. Lett. **26,** 1019–1021 (2001).
12. S. Mookherjea and A. Yariv "Second harmonic generation with pulses in a coupled-resonator optical waveguide," Phys. Rev. E **65,** (2002).
13. S. Blair "Nonlinear sensitivity enhancement with one-dimensional photonic bandgap microcavity arrays," Opt. Lett. **27,** 613–615 (2002).
14. M. Soljacic, S. G. Johnson, S. Fan, M. Ibanescu, E. Ippen, and J. D. Joannopoulos "Photonic crystal slow-light enhancement of nonlinear phase sensitivity," J. Opt. Soc. Am. B **19,** 2052–2059 (2002).
15. S. Blair "Self-focusing of narrow one-dimensional beams in photonic microcavity arrays," J. Opt. Soc. Am. B **20,** 1520-1526 (2003).

#7063 - $15.00 US
Received 5 April 2005; revised 10 May 2005; accepted 10 May 2005

16. G. Priem, I. Notebaert, B. Maes, P. Bienstman, G. Morthier, and R. Baets "Design of all-optical nonlinear functionalities based on resonators," IEEE J. Sel. Top. Quantum Electron. **10,** 1070–1078 (2004).
17. G. Priem, I. Notebaert, P. Bienstman, G. Morthier, and R. Baets "Resonator-based all-optical Kerr-nonlinear phase shifting: design and limitations," J. Appl. Phys. **97,** 023104 (2005).
18. D. J. Ripin, K.-Y. Lim, G. S. Petrich, P. R. Villeneuve, S. Fan, E. R. Thoen, J. D. Joannopoulos, E. P. Ippen, and L. A. Kolodziejski "Photonic band gap airbridge microcavity resonances in GaAs/Al_xO_y waveguides," J. Appl. Phys. **87,** 1578–1580 (2000).
19. M. J. Steel and C. M. de Sterke "Parametric amplification of short pulses in optical fiber Bragg gratings," Phys. Rev. E **54,** 4271–4284 (1996).
20. T. Hattori, N. Tsurumachi, and H. Nakatsuka "Analysis of optical nonlinearity by defect states in one-dimensional photonic crystals," J. Opt. Soc. Am. B **14,** 348–355 (1997).
21. N. Tsurumachi, S. Yamashita, N. Muroi, T. Fuji, T. Hattori, and H. Nakatsuka "Enhancement of nonlinear optical effect in one-dimensional photonic crystal structures," Jpn. J. Appl. Phys. **38,** 6302–6308 (1999).
22. G. J. Schneider and G. H. Watson "Nonlinear optical spectroscopy in one-dimensional photonic crystals," Appl. Phys. Lett. **83,** 5350–5352 (2003).
23. A. Melloni, F. Morichetti, and M. Martinelli "Optical slow wave structures," Opt. Photon. News **14,** 44–48 (2003).
24. Y. Chen and S. Blair "Nonlinearity enhancement in finite coupled-resonator slow-light waveguides," Opt. Express **12,** 3353–3366 (2004).
25. Y. Chen, G. Pasrija, B. Farhang-Boroujeny, and S. Blair "Engineering the nonlinear phase shift using multi-stage auto-regressive moving-average optical filters," Appl. Opt. **13,** 2564–2574 (2005).

1. Introduction

The notion of the photonic crystal [1, 2] has generated tremendous research interest in recent years. Of particular importance is the photonic crystal defect, which opens up density of states within the bandgap and facilitates a number of useful devices [3, 4] such as waveguides and lasers [5], modulators [6], and filters [7, 8] based upon high-finesse defect cavities. Coupled defects have also been proposed [9, 10] and demonstrated [11] for optical waveguiding and have been analyzed for their nonlinear properties [12, 13, 14, 15]. While the most practical embodiment of coupled-defect photonic crystal devices is the 2-D photonic crystal slab [11, 14], the essential elements of the enhancement of nonlinear processes can be studied in a 1-D layered geometry [13, 16, 17], as illustrated in Fig. 1, which has equivalence to air holes drilled in a high index waveguide [7, 18, 8], for example.

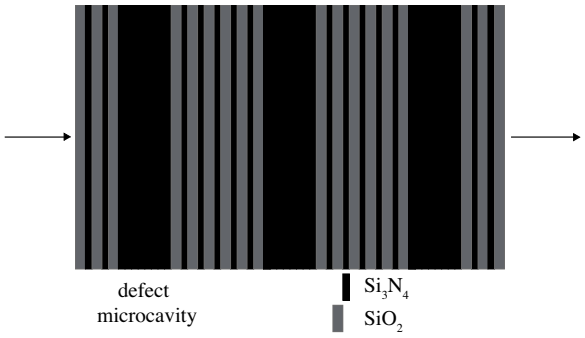

Fig. 1. One-dimensional photonic crystal coupled-defect structure. The layer sequence for this structure is given by $(\mathrm{LH})^3\left[(\mathrm{H})^7(\mathrm{LH})^6\right]^2(\mathrm{H})^7(\mathrm{LH})^2\mathrm{L}$, and consists of three coupled defects of 8 H-layers each.

The nonlinear phase shift process [13, 14, 17] and second-harmonic generation [12] have been studied in coupled-defect structures. Another important process for chip-scale photonic systems is four-wave mixing, which can be used for wavelength conversion and logical operations. While four-wave mixing has been studied in Bragg gratings [19] and Fabry-Perot (i.e.,

#7063 - $15.00 US Received 5 April 2005; revised 10 May 2005; accepted 10 May 2005

single defect) structures [20, 21, 22], it has not been studied in coupled-defect photonic crystal structures (although a related study for generic coupled-resonators, as opposed to coupled photonic crystal defects, has been reported [23]). In this paper, such studies are performed for two different situations - 1) each of the four frequencies lie at an intraband resonance and must be separated by multiples of the free-spectral range (FSR), and 2) the four frequencies lie within the mini-band resonance of a coupled-defect structure.

Results are obtained via a custom nonlinear 1-D FDTD code [13], using spatial sampling of 4 nm and time sampling of 13.3 attoseconds. Two Gaussian pulses - the pump (ω_p) and signal (ω_s) - of time duration 8.3 ps (full-width at half intensity maximum) are incident on the structure. The frequency conversion efficiency is defined as the energy of the pulse at the output of the structure at converted frequency $\omega_c = 2\omega_p - \omega_s$, divided by the energy of the signal pulse at the input. Because simulation is performed in the time domain, higher-order mixing products are also obtained, but they are weaker in magnitude than the primary mixing products at $2\omega_p - \omega_s$ and $2\omega_s - \omega_p$.

2. Four-wave mixing at intraband resonances

The first structure has a layer sequence given by

$$(\mathrm{LH})^4 \left[(\mathrm{H})^{127}(\mathrm{LH})^8\right]^2 (\mathrm{H})^{127}(\mathrm{LH})^3\mathrm{L}, \tag{1}$$

where L and H represent quarter-wave layers near 800 nm wavelength of low and high refractive index, respectively; the three defect cavities consist of 128 H-layers each. The refractive indices of 1.46 and 2.1 correspond to SiO_2 and Si_3N_4, respectively and the physical length is 42.0 μm; without defects, the width of the bandgap would be 188 nm. With this coupled-defect structure, the intraband resonance FSR is 11.95 nm, so that λ_p=794.25 nm and λ_s=806.20 nm and the converted wavelength is at λ_c=782.65 nm. The linear transmission spectrum is shown in Fig. 2 with the two central resonances excited the by the pump and signal waves. Even though

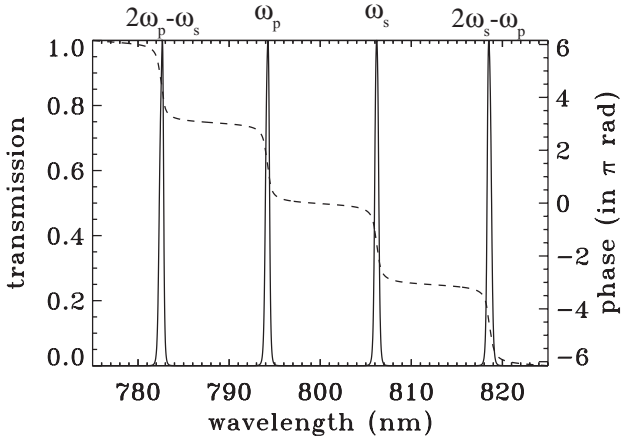

Fig. 2. Linear transmission spectra of the coupled-defect structure of equation 1 showing the mangitude transmission (solid linestyle) and phase (dashed linestyle) of the intraband resonances.

the structure defined by Eq. (1) contains three coupled defects, the intraband transmission resonances consist of single transmission peaks (i.e., no miniband) with greater group delay than

#7063 - $15.00 US
Received 5 April 2005; revised 10 May 2005; accepted 10 May 2005

that of the corresponding single defect structure of the same quality factor. The resonance quality factor is about 1700 and the initial phase mismatch $\Delta\phi = (2\phi_p - \phi_s) - \phi_c$ at the converted wavelength is about 0.005π.

Figure 3 shows the frequency conversion efficiency as a function of pump intensity normalized to the nonlinear refractive index. The pump to signal intensity ratio $I_p/I_s = 10$ (equivalent to the ratio of initial pulse energies). Also plotted in the figure are the conversion efficiencies of a bulk material of the same length and of a single defect structure. At low input intensity, the conversion efficiency of the coupled-defect structure is about 1500-times greater than the bulk material, demonstrating the advantage of slow-light enhancement (the group delay for the defect structure is 2.47 ps at the pump frequency versus 0.29 ps for the bulk). In addition, compared to the single defect structure (with quality factor of 1940, group delay of 1.66 ps, and physical length 14.9 μm), the coupled-defect structure has 1.9 times greater conversion efficiency. At high input intensities, the four-wave mixing response of the coupled-defect structure peaks at about 5%, then decreases, due to nonlinear detuning, such that the advantage over the bulk material lessens (note that the single defect structure peaks at lower intensity than the multi-defect structure). The effect of nonlinear detuning of the resonance is that the pulse spectra become clipped due to the sharp falloff of the resonance lineshapes, thereby reducing the energy transmitted to the output. Longer initial pulse durations (i.e. quasi-cw) would reduce this clipping (in fact, the ratio of peak pulse intensities shows saturation but not rolloff over the pump input intensity range). With coupled defect structures, an additional effect arises in the change of $\Delta\phi$ with detuning, as the nonlinear refractive index change is not the same across all defects [13], thereby distorting the initial linear transfer function shape. The use of flat-topped resonances (enabled by modifying the effective coupling coeffients between defects) can significantly reduce the detrimental effects of detuning [24, 25].

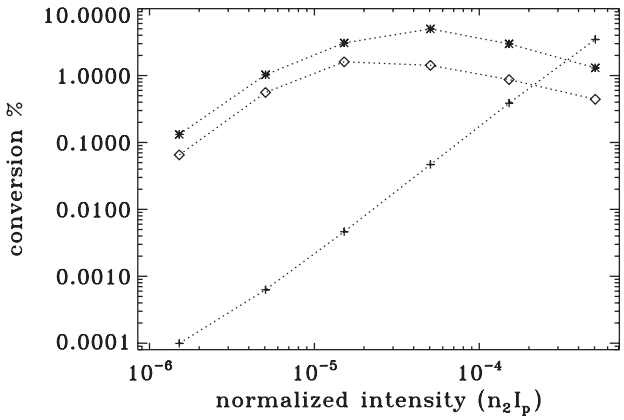

Fig. 3. Frequency conversion efficiency for a structure with layer sequence given by equation 1 (data points indicated by '*'), a bulk layer of equal thickness 440 H (data points indicated by '+'), and single defect structure of the form $(LH)^6H^{127}(LH)^5L$ (data points indicated by diamonds). The initial pump to signal intensity ratio is 10.

By using intraband resonances, the only means to decrease the wavelength spacing is to increase the defect cavity length. With a length of 256 H-layers, the FSR decreases to 6.05 nm, and the physical length increases to 78.9 μm. (For a cavity length of 1536 H, the FSR is about 1 nm with physical length of 450 μm). In addition, the quality factor and group delay increase to $Q \sim 3300$ and 4.86 ps. At low input intensities, the enhancement over the bulk material (of 0.55 ps group delay) is about 1200, and again the four-wave mixing response rolls over at high

#7063 - $15.00 US
Received 5 April 2005; revised 10 May 2005; accepted 10 May 2005

intensities, as shown in Fig. 4, with a peak of 6.4%.

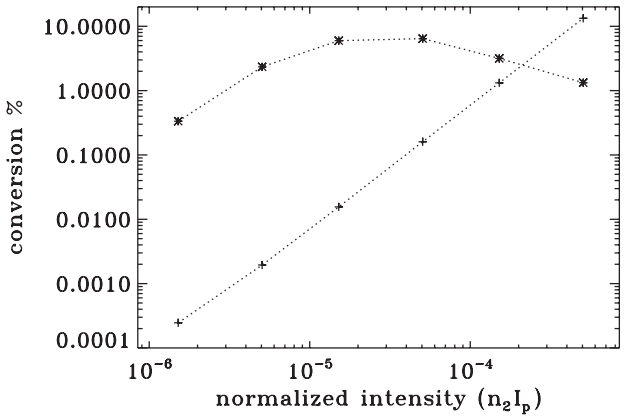

Fig. 4. Frequency conversion efficiency for a structure with three coupled defects and defect cavity length of 256 H (data points indicated by '*') and a bulk layer of equal thickness 828 H (data points indicated by '+'). The initial pump to signal intensity ratio is 10.

3. Four-wave mixing by miniband resonances

With intraband resonances, very long defect cavities are necessary in order to perform frequency conversion with narrow frequency spacing as the FSR is primarily determined by the length of the defect and depends weakly on the mirror layers and the number of defects. Small frequency spacing can alternatively be realized by using the miniband resonances associated with coupled-defect structures.

Consider the following generalized structure

$$(\mathrm{LH})^M \left[\mathrm{H}\,(\mathrm{LH})^M\right]^{N-1} \mathrm{H}\,(\mathrm{LH})^{M-1}\,\mathrm{L}, \tag{2}$$

where M is the number of mirror LH pairs and N is the number of defects of length 2 H. In this structure, the miniband has N resonance peaks; as N increases, the overall widths (and spacings) of the intraband resonances remain nearly constant but the widths and spacings of the miniband resonances decrease. Alternatively, if N is constant and M increases, the spacings of the intraband resonances remain nearly constant, but the widths of the intraband resonances decrease with constant number of miniband peaks.

The first case is $M = 5$ and $N = 8$, where the linear transmission versus wavelength is shown in Fig. 5. The pump and signal wavelengths are $\lambda_p = 796.35$ nm and $\lambda_s = 805.05$ nm, and the converted wavelength is at $\lambda_c = 787.84$ nm. The physical length of the structure is 11.1 μm, while the minimum wavelength spacing is 8.7 nm; the initial phase mismatch at the converted frequency is 0.09 π and the linear transmission is 94.4%. Figure 6 plots the conversion efficiency for this structure versus normalized pump intensity. Also plotted is the efficiency for a bulk material of the same physical length, which shows that the coupled-defect structure has 30 times greater conversion efficiency at low pump inputs. The group delay of the coupled-defect structure is 200 fs versus 78 fs for the bulk material, calculated at the pump frequency. As before, at high pump intensities, the conversion efficiency saturates, but the effect is not as severe as in the intraband resonance case because the transmission between the central miniband resonances does not drop to zero for this structure, implying that spectral clipping upon detuning is reduced.

#7063 - $15.00 US Received 5 April 2005; revised 10 May 2005; accepted 10 May 2005

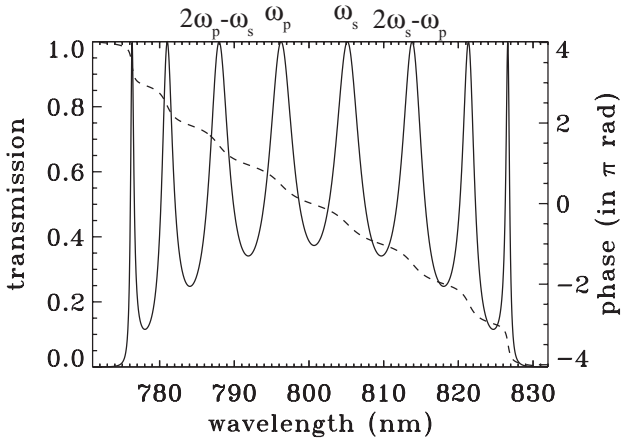

Fig. 5. Linear transmission spectra of the coupled-defect structure of equation 2 (with $M = 5$ and $N = 8$) showing the transmission magnitude (solid linestyle) and phase (dashed linestyle) of the central miniband resonances.

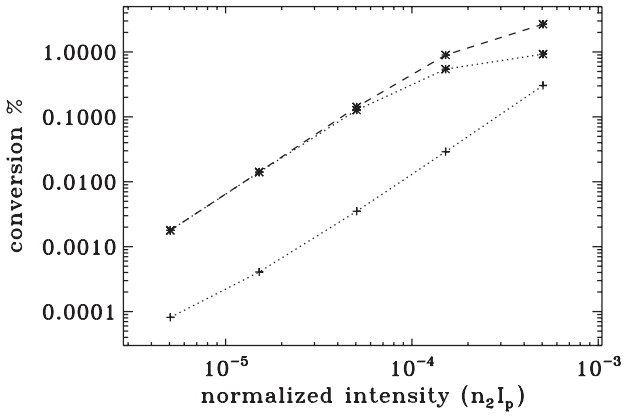

Fig. 6. Frequency conversion efficiency for a structure with layer sequence given by equation 2 with $M = 5$ and $N = 8$ (data points indicated by '*', pump to signal intensity ratio of 10 connected by dashed lines, ratio of 1 connected by dotted lines) and a bulk layer of equal thickness 116 H (data points indicated by '+').

As Fig. 6 shows, the conversion efficiency is greater for higher pump to signal intensity ratio. This is to be expected as lower signal intensity reduces the amount of detuning. It is also interesting to plot conversion efficiency versus pump to signal intensity ratio, Fig. 7, which further illustrates this effect. At low conversion efficiencies, the variation with ratio is not significant, but it is clear that the conversion saturates (at about 0.146% in this case) at high ratios; at pump intensities closer to maximum conversion, the variation more significant. In this paper, an initial ratio of 10 is chosen for all simulation results throughout.

The pump and signal frequency spacing can be reduced by increasing the number of mirror pairs M. Table 1 lists the relevant parameters as a function of M, with $N = 8$. Using a pump to signal intensity ratio of 10, Fig. 8 plots the conversion efficiency as a function of M. Due to nonlinear detuning, the maximum conversion efficiency is limited to about 1%, which occurs at high pump intensity for small M, and lower pump intensities for larger M. The detrimental

#7063 - $15.00 US
Received 5 April 2005; revised 10 May 2005; accepted 10 May 2005

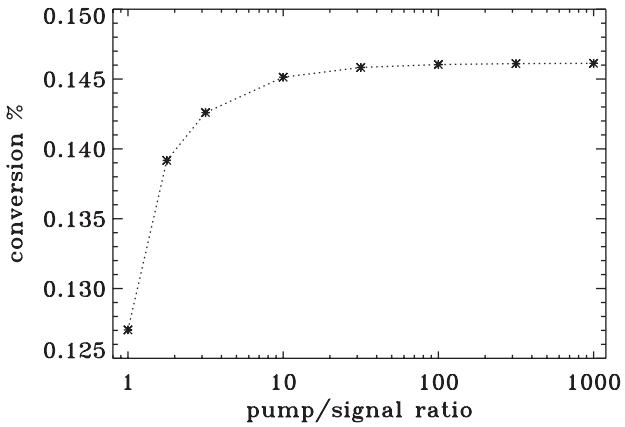

Fig. 7. Frequency conversion efficiency for a structure with layer sequence given by equation 2 with $M = 5$ and $N = 8$ (data points indicated by '*') versus initial pump to signal intensity ratio. The normalized pump intensity $n_2 I_p = 5 \times 10^{-5}$.

effects of detuning can clearly be seen for larger M because, as M increases, the isolation between miniband resonances increases. Note also that, in addition to the lower group delay as compared to the intraband resonance case for the same minimum frequency spacing, the overall conversion efficiency is limited by the fact that the mixing products don't fall exactly on resonance peaks of the miniband (because the miniband peaks are not uniformly spaced in frequency like the intraband resonance peaks [24]), thus increasing the phase mismatch and reducing the transmission.

Table 1. Linear parameters for coupled-defect structures of equation 2 with $N = 8$.

M	min. spacing	phys. length	group delay
4	12.85 nm	9.0 μm	104 fs
5	8.70 nm	11.1 μm	200 fs
6	6.06 nm	13.2 μm	400 fs
7	4.20 nm	15.3 μm	810 fs
8	2.89 nm	17.4 μm	1.64 ps
9	2.01 nm	19.6 μm	3.42 ps

When using miniband resonances, another way to decrease the frequency spacing is to increase the number of defects N. Table 2 shows how the spacing, physical structure length, and group delay change with N, and Fig. 9 plots the conversion efficiency for these structures. Note by comparison that increasing M is more efficient in terms of reducing the minimum frequency spacing and increasing group delay within a compact structure (for example, compare $M = 7$ from Table 1 to $N = 16$ from Table 2). However, saturation and rolloff of the conversion efficiency is not as apparent as N is increased, mainly because the intensity buildup is not as high as for structures with larger values of M, and as the number of resonances within the miniband increases, the overlap between them also increases. In addition, the central miniband resonances become more nearly uniformly spaced in frequency as N increases. It should be clear that there are combinations of M and N that can produce high sensitivity and large overall conversion.

#7063 - $15.00 US
Received 5 April 2005; revised 10 May 2005; accepted 10 May 2005

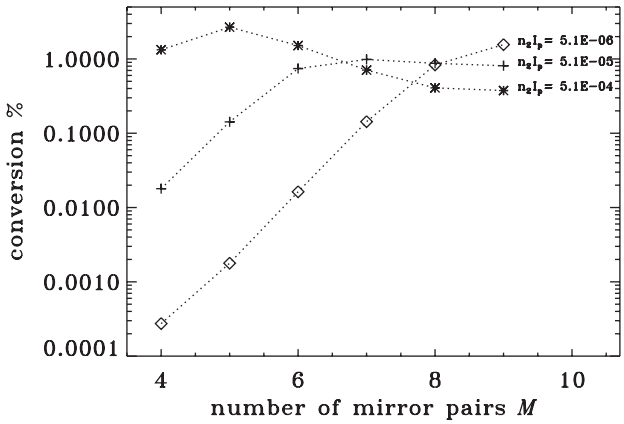

Fig. 8. Frequency conversion efficiency for a structure with layer sequence given by equation 2 with $N = 8$ versus the number of mirror pairs M. The efficiency is plotted at three different pump intensity levels. The initial pump to signal intensity ratio is 10.

Table 2. Linear parameters for coupled-defect structure of equation 2 with $M = 5$.

N	min. spacing	phys. length	group delay
4	15.6 nm	6.1 μm	115 fs
8	8.70 nm	11.1 μm	200 fs
12	6.13 nm	16.1 μm	283 fs
16	4.74 nm	21.2 μm	370 fs

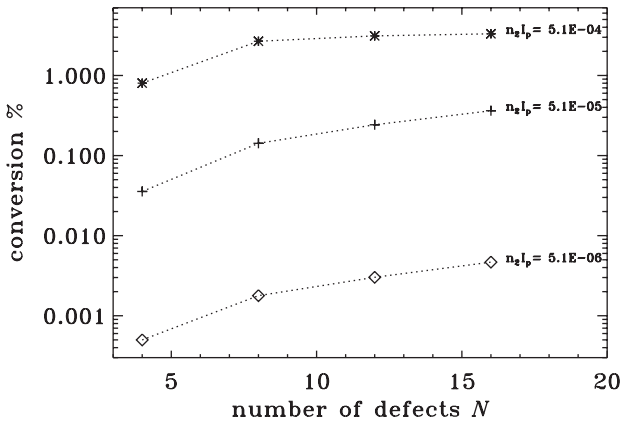

Fig. 9. Frequency conversion efficiency for a structure with layer sequence given by equation 2 with $M = 5$ as a function of the number of defects. The efficiency is plotted at three different pump intensity levels. The initial pump to signal intensity ratio is 10.

#7063 - $15.00 US
Received 5 April 2005; revised 10 May 2005; accepted 10 May 2005

4. Conclusion

Frequency conversion efficiency via four-wave mixing can be significantly increased over bulk material by using photonic crystal coupled-detect structures. The greatest efficiency is obtained through the use of intraband resonances (greater than 5% overall conversion, 1000x greater sensitivity), but small frequency spacings require long defect lengths. An alternative is to use the miniband resonances of coupled-defect structures, where $\sim$ half-wave length defects can be employed, resulting in significant decrease in overall structure length for the same frequency spacing. The tradeoff is a reduction in sensitivity (with a peak conversion efficiency of a few %), resulting in part to the lower group delay associated with the miniband resonances for the same minimum frequency spacing.

#7063 - $15.00 US
Received 5 April 2005; revised 10 May 2005; accepted 10 May 2005